SF2A 2024
M. Béthermin, K. Baillié, N. Lagarde, J. Malzac, R.-M. Ouazzani, J. Richard, O. Venot, A. Siebert (eds)

DISCOVERY OF A NEW STREAMER AROUND THE CLASS I YSO L1489 IRS: MODELING AND CONSEQUENCES

M. Tanious[1,2], R. Le Gal[1,2] and A. Faure[1]

Abstract. The interstellar heritage of planetary systems remains poorly understood, especially during the crucial Class I stage of star formation. During this phase, a young protostar continues to accrete material from its surrounding envelope, and the chemical composition of this material plays a key role in shaping the future planetary system. An ideal target to study the interstellar heritage question is L1489 IRS, a Class I protostar embedded in its parental molecular cloud. We conducted a 3mm-survey using the NOEMA interferometer to explore both the chemistry and structures around this young stellar object. We identified a new streamer, likely responsible for the warp disk in this system, and probably associated with accretion shocks at the landing point of the streamer on the disk. This work opens the door to further observational and modeling studies of this source.

Keywords: Stars: low-mass, Protoplanetary disks, Astrochemistry, ISM: lines, ISM: dynamics

1 Introduction

During the process of star formation, the region surrounding the star undergoes significant changes. As these regions are known to host a rich chemistry, this raises the question of interstellar inheritance: how many molecules from the parental molecular cloud survive the star formation process and are passed on to the forming planetary system? Several studies focused on the early Class 0 phase – for instance TIMASSS (Caux et al. 2011), PILS (Jørgensen et al. 2016), ASAI (Lefloch et al. 2018), SOLIS (Ceccarelli et al. 2017), GEMS (Fuente et al. 2019) – or the later Class II stage – such as DISCS (Öberg et al. 2010, 2011a), CID (Guilloteau et al. 2016), MAPS (Öberg et al. 2021). While the ALMA Large Programs FAUST (Codella et al. 2021) and eDisk (Ohashi et al. 2023) have begun to investigate the chemistry and the dust substructures within Class 0/I disks at high spatial resolution, there are still few studies that have examined the interstellar inheritance at the Class I stage. A pilot study using the IRAM-30m telescope revealed the chemical richness of seven Class I protostellar systems (Le Gal et al. 2020). Among this sample, L1489 IRS (a.k.a. IRAS 04016+2610) is particularly notable for being embedded in its parent molecular cloud, Barnard 207 (Togi et al. 2017). This system has been observed multiple time with interferometers including the SMA (Brinch et al. 2007b; Yen et al. 2013) and ALMA (Yen et al. 2014; van't Hoff et al. 2020; Sai et al. 2020; Tychoniec et al. 2021; Yamato et al. 2023). However, most studies have focused on CO and its isotopologues, or 1mm lines. To address this gap, we conducted observations using the NOEMA interferometer targeting the 3mm band toward L1489 IRS.

2 Observations

2.1 Overview

Figure 1 shows the integrated intensity (moment 0) maps from the combined NOEMA and IRAM-30m data for some of the 10 brightest lines in the 3mm survey (adapted from Tanious et al. 2024). A variety of structures are clearly visible: cold and dense gas, known to be probed with HCO^+ and CS, is particularly useful to identify the envelope and potential outflows. SO acts as a molecular tracer of shocks (e.g., Garufi et al. 2022, and references therein), or can witness fresh material (e.g., Hacar & Tafalla 2011, and references therein). Finally, cavity walls are traced with C_2H (Tychoniec et al. 2021), and HC_3N is a characteristic marker of infalling material like "accretion streamers" (Pineda et al. 2020).

[1] Université Grenoble Alpes, CNRS, IPAG, F-38000 Grenoble, France
[2] IRAM, 300 rue de la piscine, F-38406 Saint-Martin d'Hères, France

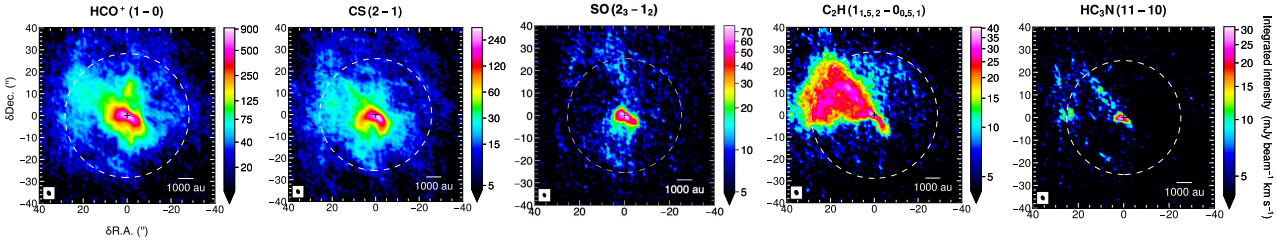

Fig. 1. Integrated intensity maps of selected lines of the 3mm survey (adapted from Tanious et al. 2024). The color scale is stretched by the arcsinh function to enhance the visibility of faint, extended features. The minimum is set to 3σ emission. For each panel, the synthesized beam of the line is shown in the lower left corner, the primary beam with a white dashed circle, and a scale bar of 1000 au is displayed on the bottom right corner.

2.2 Outflow

A bipolar outflow stands out in HCO^+ $(1-0)$ emission, with the blue lobe extending to the south, and the red lob to the north, with a Position Angle (P.A) of $-8°$ (Tanious et al. 2024). It is perfectly perpendicular to the innermost disk in this system with a P.A. of $82°$ (Yamato et al. 2023). We retrieve the same shape as identified in $CO(2-1)$ emission (Yen et al. 2014), apart from the northwestern part of the V-shaped red lobe (PA $= -60°$). If its velocity range is not broad enough, this HCO^+ emission may simply be hidden in the envelope.

2.3 Quadrupolar flow

In H_2 $(1-0)$ S(1) observations at 2.12 μm, obtained with the United Kingdom Infrared Telescope (UKIRT), a quadrupolar flow-like structure was identified, with the two major axes labeled as "primary" and "secondary" (Lucas et al. 2000). They are even better seen in the polarized intensity image at 2.2 μm (see Fig. 2 left panel) and where interpreted as outflows, as the map suggests the presence of bow shocks (Lucas et al. 2000). We recover this quadrupolar structure in the blue-shifted emission of CS, as shown in Fig. 2 right panel. Notably, HC_3N emission is elongated along the secondary axis, which is more commonly considered in the literature as a tracer of infalling material, or streamers (Pineda et al. 2020). To distinguish between outflow or streamer, we ran two models of infalling material and attempted to fit the results to the data.

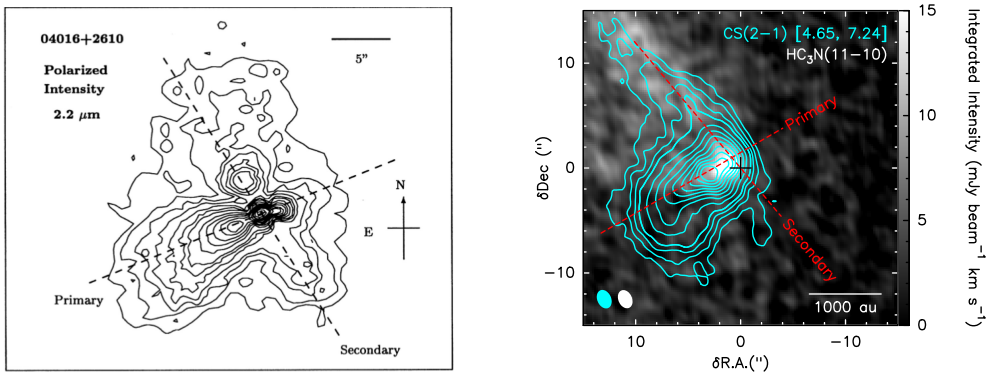

Fig. 2. Left: Polarized intensity emission at 2.2 μm obtained with the UKIRT (Fig.2 from Lucas et al. 2000). **Right:** Integrated intensity emission of HC_3N (background) and blue-shifted integrated intensity emission of CS (contours). The contour levels are 30σ to 45σ by 5σ steps then 45σ to 125σ by 10σ steps where $\sigma = 1.0$ mJy beam^{-1} km s^{-1}. The two axes of the quadrupolar flow are denoted with dashed red lines. The synthesized beams are displayed in the lower left corner. A scale bar of 1 000 au is shown on the bottom right corner (Fig. 6 from Tanious et al. 2024).

3 Infall models

3.1 Streamline model

The model is based on the Newtonian analytic solutions of infalling material, within a rotating cloud, moving in free-fall motion toward a central object (Mendoza et al. 2009). We used the version implemented by Pineda et al. (2020) which takes as input: the initial position (r_0, θ_0, φ_0) and radial velocity $v_{r,0}$ of the infalling mass in spherical coordinates, the mass of the central object $M_\star$, the initial angular velocity of the cloud Ω_0, and the rotational axis. As no value of Ω_0 was available in the literature, we derived it from the centrifugal radius used in the disk-to-envelope model of Sai et al. (2022) with the star mass taken as 1.7 $M_\odot$ (Yamato et al. 2023). We varied initial positions and radial velocities along a grid, and tested three different rotational axis (Tanious et al. 2024). A visual inspection was then carried out to identify the best-fitting parameters for the observations.

Along the primary axis, we encountered difficulties in finding parameters that simultaneously fit both the emission and velocity profile, leading us to conclude that it is unlikely to be a streamer. Interestingly, this axis aligns well with the missing red-shifted component of the outflow seen in CO(2 − 1) emission (cf. Sect. 2.2). The blue-shifted component seen in CS emission could thus be the blue-lobe of this second outflow (Tanious et al. 2024). New NOEMA observations that we conducted at 1mm at high spatial resolution gives hint of a more collimated blue-shifted CS (5 − 4) emission along this primary axis, supporting this hypothesis (Tanious et al., in prep). If two outflows are indeed present, this would serve as a strong indicator of the system's presumed binarity (Hogerheijde & Sandell 2000; Brinch et al. 2007b).

Along the secondary axis though, multiple parameters fit the observations indicating that the emission is likely coming from a streamer (Tanious et al. 2024). The best fit is shown on Fig. 3 left panel.

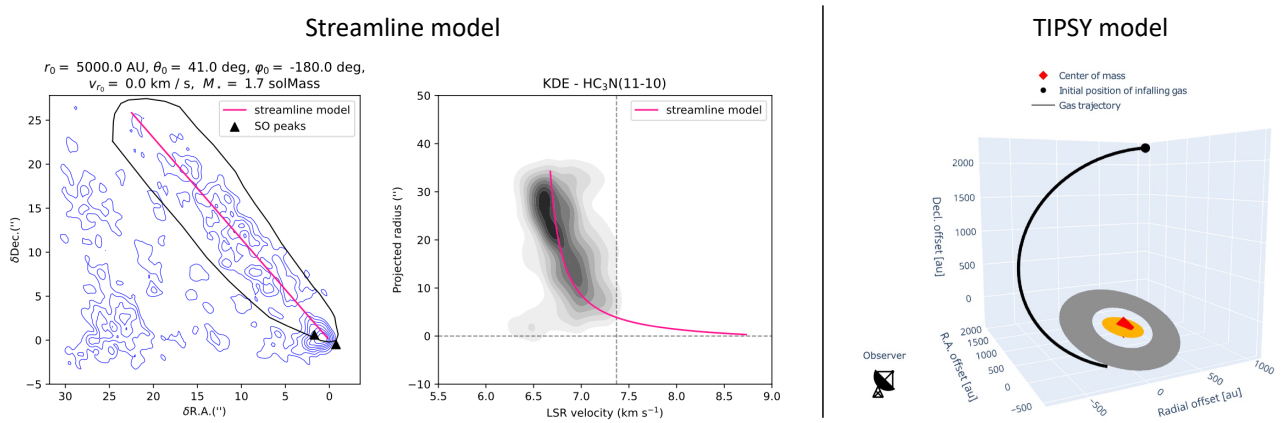

Fig. 3. Left: Streamline model of the HC_3N blue-shifted for the best set of parameters in pink. The left panel shows the HC_3N blue-shifted integrated emission (background), while the right panel shows an estimation of the velocity profile from the data (background). Adapted from Tanious et al. (2024). **Right:** Trajectory computed by `TIPSY` from the HC_3N PPV cube. The intermediate and outer disks are displayed in orange and grey (Sai et al. 2020). Adapted from Tanious et al. (2024).

3.2 TIPSY model

`TIPSY` (Trajectory of Infalling Particles in Streamers around Young stars) is a new Python package based on a more general form of the equations of Mendoza et al. (2009). It is designed to directly fit position-position-velocity (PPV) cube, which serve as one of the model's inputs (Gupta et al. 2024). The other inputs include the mass of the central object (taken as 1.7 $M_\odot$, like in Sect. 3.1), the distance to the object (146 pc, Roccatagliata et al. 2020), and the systemic velocity of the source (7.37 km s^{-1}, Yamato et al. 2023).

Like the streamline model, `TIPSY` cannot fit the observations along the primary axis, but is able to converge on the secondary axis, resulting in a 3320 ± 165 au-long streamer. It is important to note that this value is underestimated, as we are missing emission located beyond NOEMA's primary beam. A 3D visualization of the trajectory is presented on Fig. 3 right panel.

4 Streamer implications

The streamer identified along the secondary axis appears to emerge from the nearby dense core L1489, located $\sim$ 7000 au from the source. It would act as a material reservoir, feeding the young protostar L1489 IRS. The connection between the core and the protostar nevertheless remains to be confirmed as the emission extends beyond NOEMA's primary beam (Tanious et al. 2024). Ongoing mosaic observations with NOEMA will help verify the existence of this connection (Tanious et al., in prep).

This system is known to have an external warped disk (Brinch et al. 2007a; Sai et al. 2020; Yamato et al. 2023), although its origin is still under debate. We propose that it was formed through material transported by the newly identified streamer (Tanious et al. 2024), as hydro-dynamical numerical simulations can reproduce such scenarios given a sufficient infall rate (Kuffmeier et al. 2021), a topic that will be discussed in a forthcoming paper (Tanious et al, in prep.).

Finally, we identified peaks in SO emission at the streamer's landing on the disk. The modeled trajectory reveals that the streamer impacts the disk's midplane assuming an aspect ratio $z/r \geq 0.4$ (Tanious et al. 2024). This supports the idea of accretion shocks occurring at these locations, as noted by Yen et al. (2014) using the SO $(5_6 - 4_5)$ line, having a higher upper energy than the presented line ($E_{\rm up} = 50.7$ K and 19.3 K respectively).

5 Conclusions

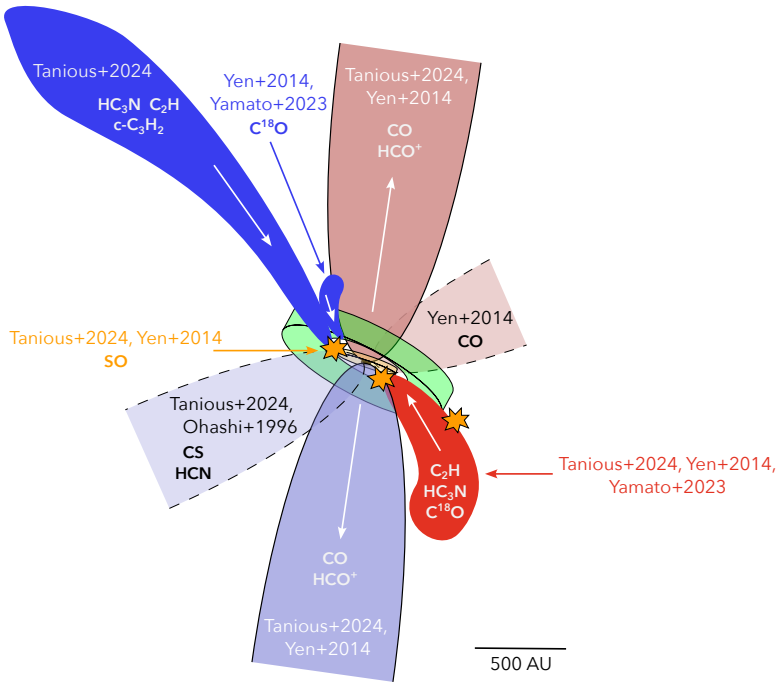

Fig. 4. The L1489 IRS system sketched and simplified at scale. The inner disk is drawn in orange, the intermediate disk in yellow, and the external warped disk in green. Red (respectively blue) colored structures correspond to red-shifted (respectively blue-shifted) emissions. The direction of moving material is indicated with white arrows. The accretion shocks are represented in orange. Dashed contours represent the potential second outflow along the primary axis. Adapted from Tanious et al. (2024).

This work enabled to confirm previously seen and identify new structures around L1489 IRS, thanks to the diverse molecular tracers from this 3mm-survey conducted with NOEMA (cf Fig. 4). Among these, a new $\geq$ 3000 au streamer as been observed in HC_3N emission, as well as other carbon-chain species (e.g. C_2H and c$-C_3H_2$). This streamer likely connects the nearby core to the protostar via a gas bridge and may be responsible for the external warped disk in the system. It is likely landing in the midplane of the disk, resulting in accretion shocks seen in SO emission. Multiple investigations are currently ongoing to confirm the connection between the nearby core and the protostar, to assess the infall rate of the streamer and its role in the warp disk origin, and explore the potential second outflow that would confirm the binarity of this system (Tanious et al., in preps).

M.T. and R.L.G thank the IRAM staff for their invaluable work making these observations possible. This work is based on observations carried out under project numbers 184-20, S20AH and W20AJ (PI: R. Le Gal), with the IRAM-30m and IRAM Interferometer NOEMA. IRAM is supported by INSU/CNRS (France), MPG (Germany) and IGN (Spain). This work was supported by the Programme National "Physique et Chimie du Milieu Interstellaire" (PCMI) of CNRS/INSU with INC/INP co-funded by CEA and CNES. This research has benefited from the Core2disk-III residential program of Institut Pascal at Université Paris-Saclay, with the support of the program "Investissements d'avenir" ANR-11-IDEX-0003-01. This project has received funding from the European Research Council (ERC) under the European Union Horizon Europe programme (grant agreement No. 101042275, project Stellar-MADE).

References

Brinch, C., Crapsi, A., Hogerheijde, M. R., & Jørgensen, J. K. 2007a, A&A, 461, 1037
Brinch, C., Crapsi, A., Jørgensen, J. K., Hogerheijde, M. R., & Hill, T. 2007b, A&A, 475, 915
Caux, E., Kahane, C., Castets, A., et al. 2011, A&A, 532, A23
Ceccarelli, C., Caselli, P., Fontani, F., et al. 2017, ApJ, 850, 176
Codella, C., Ceccarelli, C., Chandler, C., et al. 2021, Frontiers in Astronomy and Space Sciences, 8, 227
Fuente, A., Navarro, D. G., Caselli, P., et al. 2019, A&A, 624, A105
Garufi, A., Podio, L., Codella, C., et al. 2022, A&A, 658, A104
Guilloteau, S., Reboussin, L., Dutrey, A., et al. 2016, A&A, 592, A124
Gupta, A., Miotello, A., Williams, J. P., et al. 2024, A&A, 683, A133
Hacar, A. & Tafalla, M. 2011, A&A, 533, A34
Hogerheijde, M. R. & Sandell, G. 2000, ApJ, 534, 880
Jørgensen, J. K., van der Wiel, M. H. D., Coutens, A., et al. 2016, A&A, 595, A117
Kuffmeier, M., Dullemond, C. P., Reissl, S., & Goicovic, F. G. 2021, A&A, 656, A161
Le Gal, R., Öberg, K. I., Huang, J., et al. 2020, ApJ, 898, 131
Lefloch, B., Bachiller, R., Ceccarelli, C., et al. 2018, MNRAS, 477, 4792
Lucas, P. W., Blundell, K. M., & Roche, P. F. 2000, MNRAS, 318, 526
Mendoza, S., Tejeda, E., & Nagel, E. 2009, MNRAS, 393, 579
Öberg, K. I., Guzmán, V. V., Walsh, C., et al. 2021, ApJS, 257, 1
Öberg, K. I., Qi, C., Fogel, J. K. J., et al. 2010, ApJ, 720, 480
Öberg, K. I., Qi, C., Fogel, J. K. J., et al. 2011a, ApJ, 734, 98
Ohashi, N., Tobin, J. J., Jørgensen, J. K., et al. 2023, ApJ, 951, 8
Pineda, J. E., Segura-Cox, D., Caselli, P., et al. 2020, Nature Astronomy, 4, 1158
Roccatagliata, V., Franciosini, E., Sacco, G. G., Randich, S., & Sicilia-Aguilar, A. 2020, A&A, 638, A85
Sai, J., Ohashi, N., Maury, A. J., et al. 2022, ApJ, 925, 12
Sai, J., Ohashi, N., Saigo, K., et al. 2020, ApJ, 893, 51
Tanious, M., Le Gal, R., Neri, R., et al. 2024, A&A, 687, A92
Togi, A., Witt, A. N., & John, D. S. 2017, A&A, 605, A99
Tychoniec, Ł., van Dishoeck, E. F., van't Hoff, M. L. R., et al. 2021, A&A, 655, A65
van't Hoff, M. L. R., Harsono, D., Tobin, J. J., et al. 2020, ApJ, 901, 166
Yamato, Y., Aikawa, Y., Ohashi, N., et al. 2023, ApJ, 951, 11
Yen, H.-W., Takakuwa, S., Ohashi, N., et al. 2014, ApJ, 793, 1
Yen, H.-W., Takakuwa, S., Ohashi, N., & Ho, P. T. P. 2013, ApJ, 772, 22